



# Recent advances in functionalization of plasmonic nanostructures for optical sensing

Amirmostafa Amirjani<sup>1</sup> · Erfan Rahbarimehr<sup>2</sup>

Received: 10 September 2020 / Accepted: 14 January 2021 / Published online: 28 January 2021  
© The Author(s), under exclusive licence to Springer-Verlag GmbH, AT part of Springer Nature 2021

## Abstract

This review summarizes the progress that has been made in the use of nanostructured SPR-based chemical sensors and biosensors. Following an introduction into the field, a first large section covers principles of nanomaterial-based SPR sensing, mainly on methods using noble metal nanoparticles (spheres, cubes, triangular plates, etc.). The next section covers methods for functionalization of plasmonic nanostructures, with subsections on functionalization using (a) amino acids and proteins; (b) oligonucleotides, (c) organic polymers, and (d) organic compounds. Several tables are presented that give an overview on the wealth of methods and materials published. A concluding section summarizes the current status, addresses current challenges, and gives an outlook on potential future trends. This review is not intended to be a comprehensive compilation of the literature in the field but rather is a systematic overview of the state of the art in surface chemistry of plasmonic nanostructures. The ability of various ligands and receptors for functionalization of nanoparticles as well as their sensing capability is discussed.

**Keywords** Biosensors · Nanosensors · Surface chemistry · Oligonucleotides · Nanocubes · Triangular plates · Biosensor · Nanotetrahedron · Nanooctohedron

## Introduction

Environmental monitoring for rapid and accurate determination of pollutant contamination in water, soil and air is one of the most pressing issues in our age. Every year, million tons of hazardous chemicals are entering the environment; hence finding a simple, rapid, and accurate determination technique is pivotal. The mentioned hazardous compounds include heavy metals, organic and inorganic pollutants, and chemical toxins [1–3]. Currently, conventional determination methods for such analytes are atomic absorption spectroscopy (AAS), atomic emission spectroscopy (AES), inductively coupled plasma/mass spectroscopy (ICP-MS), and ultraviolet-visible (UV-Vis) spectroscopy. Despite the high sensitivity and selectivity, these methods often need high operating costs, long sample preparation time, and well-trained operators [4, 5].

Therefore, there is a multidisciplinary effort for developing chemical sensors with specific abilities such as in situ multiplexed analyte determination, portability, sensitivity, and selectivity. Chemical sensors have the ability to transform the obtained chemical information upon binding of molecular guests to analytical information through different mechanisms such as electrochemistry, fluorescence, absorption, and scattering [6–9]. Chemical sensors based on nanostructured materials have received a close attention, and among them, colorimetric sensors based on plasmonic nanostructures have gained a great interest [10–21]. Localized surface plasmon resonance (LSPR)-based sensors for rapid and accurate determination of different analytes have been sufficiently covered in the previous literatures, and it is not the scope of this review. Here in this review, we are going to focus on the surface chemistry of plasmonic nanostructures for sensing applications, which was not adequately addressed in previous studies. First, a brief introduction on the theory and background of SPR phenomenon is presented which is followed by a comprehensive review on different surface functionalizing agents. To the best of our knowledge, this aspect was not comprehensively studied by previous literatures in the field, and this extensive review can be used as a guideline for the researchers.

✉ Amirmostafa Amirjani  
Amirjani@sharif.edu

<sup>1</sup> Materials Science and Engineering Department, Sharif University of Technology, P.O. Box 11155-9466, Azadi Avenue, Tehran, Iran

<sup>2</sup> Department of Chemistry, Université de Sherbrooke, QC J1K 2R1, Canada

## Surface plasmon resonance

Conversion of photons into collective oscillation of noble metals' conduction band electrons is known as localized surface plasmon resonance. This resonance coupling has opened new applications for plasmonic nanostructures due to their extraordinary absorption and scattering profile at these specific frequencies. The resonance frequency is highly depended on size, shape, composition, and environment medium of nanostructure [22–24]. The localized plasmonic fields in the immediate vicinity of nanostructures are highly sensitive to even minor changes in their near-fields, and this is the basis for their versatile applications as plasmonic sensors.

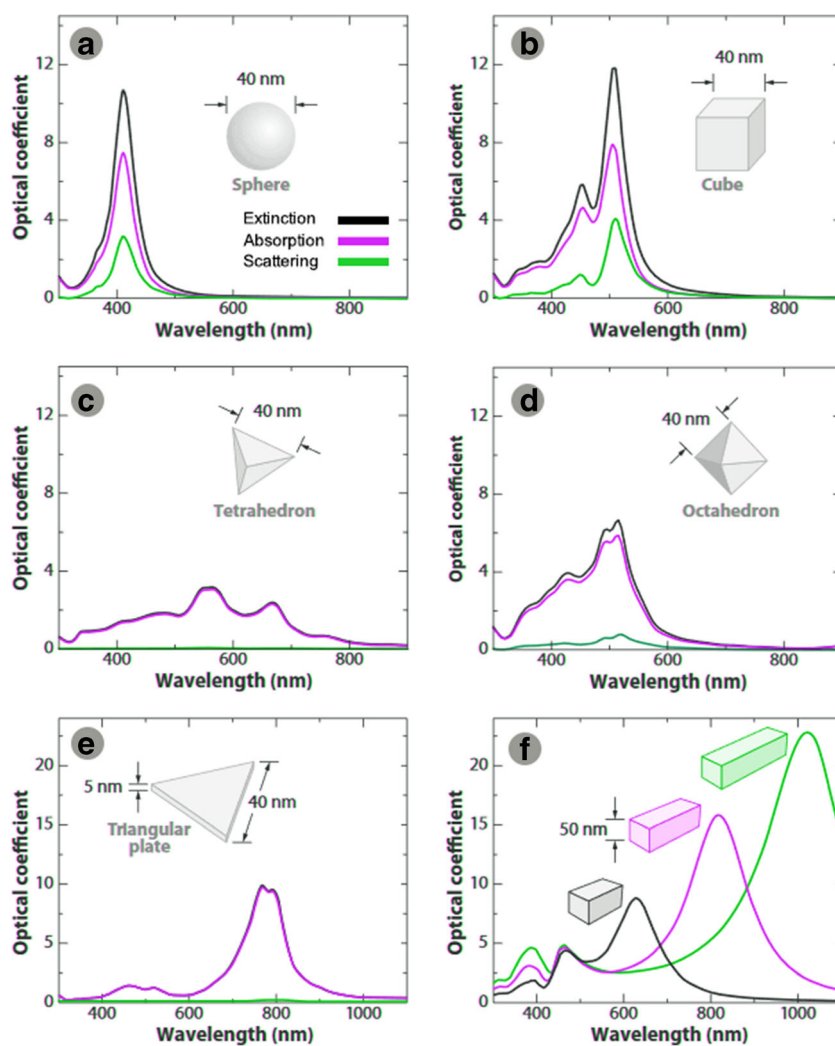
Plasmonic nanostructures have the ability to scatter or absorb light with several orders of magnitude larger than their physical sizes. In this regard, plasmonic nanostructures in different shapes and sizes were exploited largely due to their distinct optical properties even in the same composition and

size [25, 26] (see Fig. 1). Silver and gold nanostructures have been studied more in this field mainly due to their *d-d* electron transitions, which take place in visible range. The superior characteristics of silver compared with gold can be inferred from Mie's solution of Maxwell's equation for a simple spherical particle (Eq. 1):

$$C_{\text{ext}} = \frac{24N\pi^2R^3\epsilon_m^{3/2}}{\lambda n(10)} \left[ \frac{\epsilon_i}{(\epsilon_r + 2\epsilon_m)^2 + \epsilon_i^2} \right] \quad (1)$$

where  $C_{\text{ext}}$  is the extinction (absorption + elastic scattering) cross section,  $R$  is the radius of particle, and  $N$  is the electron density. Refractive index of medium, imaginary, and real terms of particle's dielectric function were also written as  $\epsilon_m$ ,  $\epsilon_i$ , and  $\epsilon_r$ , respectively. According to this equation, the maximum extinction cross-section can be obtained if both  $\epsilon_r = 2\epsilon_m$  and  $\epsilon_i \approx 0$  conditions are met. We have previously shown that imaginary part of silver's dielectric function is

**Fig. 1** Extinction (black), absorption (violet) and scattering (green) profiles of silver nanostructures with different shapes (a–f). Panel (f) shows the extinction profile of nano-bars with different aspect ratio of 2, 3, and 4 for black, violet, and green, respectively. Reproduced with permission from reference [25]



close to zero; also its imaginary part is more negative compared to gold [4]. In addition, the media in which the nanoparticles (NPs) are dispersed play a key role in their optical properties [27]. The optical extinction of the same nanoparticle in different media is not identical which can be attributed to the  $\epsilon_m$  term in Eq. 1. These changes may occur in the intensity of SPR peak or spectral shift, but the main characteristic of the spectra (number of peaks and intensity ratio among different peaks) stays the same. However, from the sensing application point of view, the medium is not a parameter of choice, so the medium is not the main point of this review but these papers are suggested in this topic [28–30].

In our previous paper, we thoroughly reviewed the different mechanisms of plasmonic sensing, e. g., aggregation-based, oxidation-based and morphological-based detection mechanisms [4]. In this review, we have focused on functionalization of plasmonic nanostructures for sensing applications. Different categories of functional agents as well as their applications for plasmonic sensing were addressed and discussed in the following sections. The functionalization strategies of plasmonic nanostructures are different, but they mainly use thiol (-SH) and amine (-NH<sub>2</sub>) groups for bonding to NP surface. Carboxylic (-COOH) and hydroxyl (-OH) groups are also used for this mean. The bonding of these groups on NPs surface is mainly described using hard and soft acid and base (HSAB) theory. Upon the interaction of functional agents with NP surface, the optical properties of NPs will change which can be observed as spectral shifts with possible decrease in the SPR peak intensity. In the following section, different functionalization strategies and the most recent works related to each category are discussed. The advantages and disadvantages of each strategy are also reviewed at the end of each section.

## Functionalizing plasmonic nanostructures for sensing applications

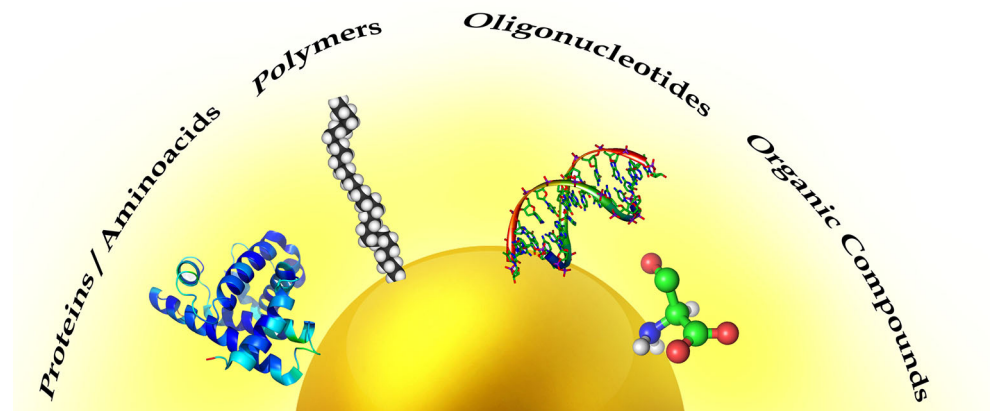
Functionalizing ligands on the surface of plasmonic nanostructures can be classified on the basis of different criteria such as the ligand composition, target analyte, and its reaction with the nanoparticle. In this review, we have emphasized on the nature of the functional ligands and categorized them in four different groups namely as oligonucleotides, proteins and amino acids, organic polymers, and organic compounds (Fig. 2). The main advantage of such approach for classification is the direct comparison of different groups' ability for sensing applications. It has been demonstrated that plasmonic nanostructures (mainly gold and silver due to their LSPR in visible region) have strong binding affinity to many chemical and biochemical compounds which makes the functionalization process robust. In the following section, different common functional groups exploited for sensing purposes will be reviewed and discussed [31].

## Functionalization using amino acids and proteins

Proteins are three-dimensional (3D) macromolecules consisting amino acids as building blocks. The 3D structure of protein highly depends on the physicochemical condition of the medium such as pH, salt concentration, and temperature [32, 33]. The size of proteins is in the range of 1–100 nm; hence they are classified as nanoparticles and are considered as ideal candidates for functionalization of nanostructures [34, 35]. Proteins have four different level structures, namely as primary, secondary, tertiary, and quaternary, which the former is the most important from the NPs interaction point of view. The primary structure of proteins which containing a set of 20 amino acids has different functional groups such as amino-NH<sub>2</sub> (lysine), carboxylic acid-COOH (aspartic, glutamic), hydroxyl-OH (serine, tyrosine), and -SH (cysteine) [36–38]. The functionalization of NPs with amino acids or proteins is usually endeavored using amine, carboxylic acid, hydroxyl, and thiol moieties available in their structures.

For instance, Jeevika et al. [39] have synthesized a colorimetric probe for determination of mercury ions by using gelatin functionalized silver nanoparticles (AgNPs) with a limit of detection of 25 nM. Upon the addition of Hg<sup>2+</sup> to the gelatin functionalized AgNP colloids, a complete color change from yellow to colorless was observed due to redox reaction between silver and mercury and led to the aggregation and formation of silver and mercury (Ag/Hg) amalgam. Zhao and colleagues [40] have introduced a colorimetric sensor based on gold nanoclusters functionalized with glutathione for the determination of Cu<sup>2+</sup> and Fe<sup>3+</sup>. The detection limits of this sensor are 0.125 and 1.25 nM for Cu<sup>2+</sup> and Fe<sup>3+</sup>, respectively. In another study, a facile and selective optical sensor based on l-cysteine capped silver nanoparticles was developed for accurate determination of Hg<sup>2+</sup> ions in aqueous solutions [26]. The synthesized AgNPs showed a high sensitivity in the range of  $1 \times 10^{-8}$  M. The selective response of l-cysteine-capped AgNPs towards Hg<sup>2+</sup> ions is shown in Fig. 3(a), where other competing metal ions are not able to interact as much as mercury. The disappearance of the S-H vibrational band in the Fourier-transform infrared spectroscopy (FTIR) of AgNPs was attributed to the anchoring of l-cysteine to the AgNP surface via a thiolate linkage. Buduru et al. [43] have developed a simple, rapid, and sensitive colorimetric method with the determination limit of 0.90  $\mu$ M for the determination of Hg<sup>2+</sup> ion in water samples using glutamine (Gln)- and histidine (His)-functionalized silver nanoparticles (Gln-His-Ag NPs) as a probe. The stretching and vibrating bands of carboxylic and amino groups of Gln and His were shifted to lower and longer wave numbers, proving the interaction of Gln and His with the surfaces of AgNPs. Tyrosine-functionalized gold nanoparticles (AuNPs) were used to develop a colorimetric probe for the determination of Cr<sup>3+</sup> and Pb<sup>2+</sup> [28]. The LOD of Cr<sup>3+</sup> and Pb<sup>2+</sup> were found to be approximately 1 and 2  $\mu$ M visually, respectively. Figure 3(b) illustrates the colorimetric sensing principle for the determination of Cr<sup>3+</sup> and Pb<sup>2+</sup> based on tyrosine-capped AuNPs. In the absence of Cr<sup>3+</sup> or Pb<sup>2+</sup>, AuNPs are well dispersed

**Fig. 2** Schematic representation of functional groups on plasmonic nanostructures for sensing application



in solution and the color of the solution remains red. Nevertheless, when  $\text{Cr}^{3+}$  or  $\text{Pb}^{2+}$  is added, their colors change from red to blue gray resulted from the aggregation of AuNPs induced by the binding between ions and tyrosine, accompanied by surface plasmon resonance (SPR) absorption peaks change in intensity and wavelength.

Ermini and co-workers [44] have synthesized peptide-functionalized gold nanoparticles as a biosensor for the determination of carcinoembryonic antigen (CEA) in blood plasma (Fig. 3(c)). It is shown that, for the same amount of target molecule, by tuning the surface properties of the peptide-functionalized NPs, it is possible to significantly enhance the sensor response for the

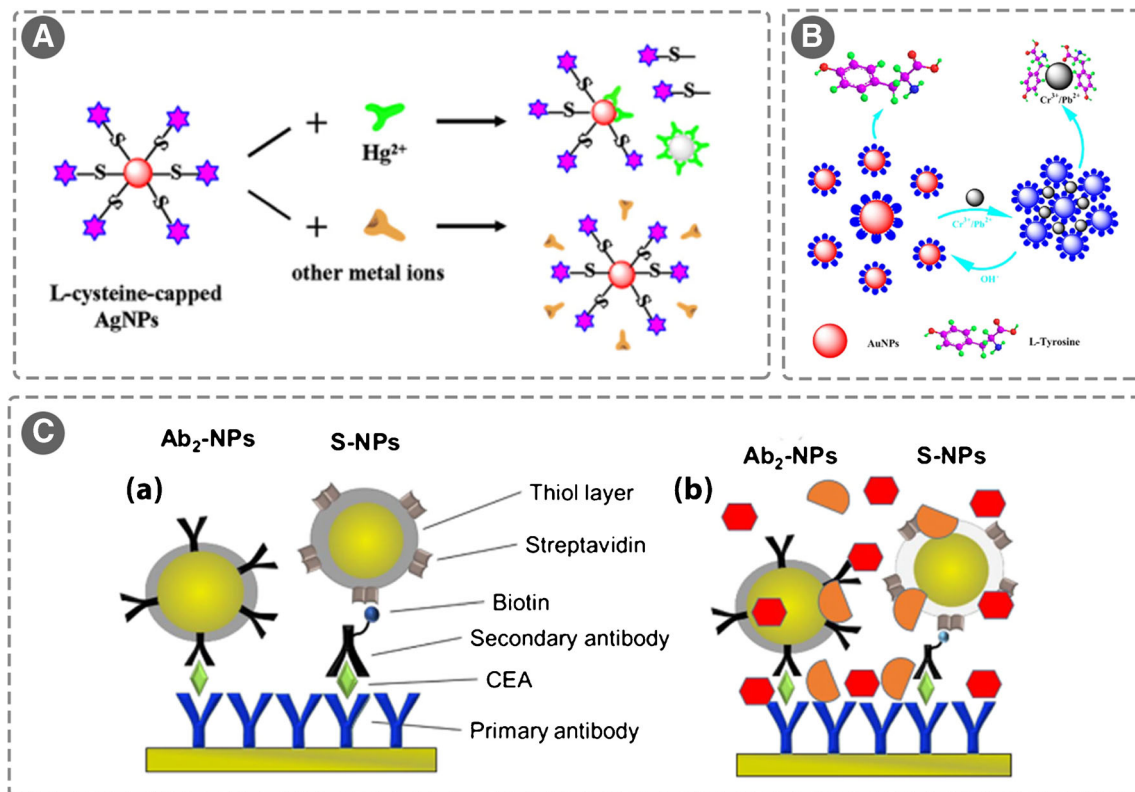


**Fig. 3** (A) Schematic representation for the selective response of L-cysteine capped AgNPs towards mercury ions. Reproduced with permission from reference [41]. (B) Schematic illustration of  $\text{Cr}^{3+}$  and  $\text{Pb}^{2+}$  detection based on optical properties of AuNPs. Reproduced with permission from reference [42]. (C) Schematic of the sandwich assays using

streptavidin functionalized NPs (S-NPs) and secondary antibody functionalized NPs ( $\text{Ab}_2$ -NPs). NPs for the determination of CEA in (a) phosphate buffer and (b) blood plasma. Reproduced with permission from reference [28]



target analyte. By using this SPR strategy, it is possible to distinguish the specific and non-specific interactions of analyte for in vivo applications. Satheeshkumar et al. [45] have proposed a label-free colorimetric assay for the determination of copper ions based on Tyrosine-functionalized silver nanoparticles with a linear range up to 10  $\mu\text{M}$ . In this study, tyrosine has been used as both reducing and functionalizing agents. A photoactive species of tyrosine (Tyr) is used to reduce silver nanoparticle through a photochemical reaction, while the oxidized Tyr (Tyr<sup>Ox</sup>) was exploited to functionalize the surface of the AgNPs at the same time. According to the FTIR measurements, the disappearance of the vibration band for phenolic C-O bending after functionalization may indicate the conversion of phenolic hydroxyl group in Tyr after photoreduction. In another study, L. D'souza and colleagues [46] have constructed a colorimetric sensor for determination of glutathione via ascorbic acid capped silver nanoparticles (AA-AgNPs) as the probe. The characteristic SPR peak of AA-AgNPs at 397 nm is redshifted to 468 nm only by the addition of a small amount of glutathione (GSH), resulting in a color change from yellow to orange-brown, which confirms the strong aggregation of AA-AgNPs by GSH due to the presence of multi-donate anchoring groups (e.g., -SH, -NH<sub>2</sub> and -COO<sup>-</sup>). The developed sensor had the ability to determine GSH in real samples. The interaction of AA molecules with AgNPs was proved by disappearance of -OH group stretching at 3212–3626  $\text{cm}^{-1}$ . Tryptophan-functionalized gold nanoparticles were used for possible applications in detecting renal function deterioration by measuring Mg<sup>2+</sup> concentrations in urine and artificial serum samples [32]. This assay has a rapid detection response of less than 1 min and a LOD of 0.2  $\mu\text{M}$ . The visual detection was accompanied by the color change from purple to dark upon the addition of Mg<sup>2+</sup>. Plasmonic nanostructures functionalized with antibodies are mostly endeavored due to their high sensitivity for detecting analytes in complex solutions. Therefore, this functionalization strategy was used for detecting several chemical and biochemical species such as atrazine, C-reactive protein, protein biomarkers, tetracycline, human immunoglobulin G (hIgG), and diphtheria toxoid [47–55]. A comprehensive list of the recent works is summarized in Table 1.

The main advantage of functionalization using proteins and amino acids is the diversity of conjugation chemistry that can be implemented for a sensing mechanism. Several moieties are available in the structure of amino acids, peptides, and proteins, and other moieties can be also grafted by straightforward conjugation reactions. Highly sensitive sensors with the detection limits down to fM or pM could be designed using antibodies due to their specific interaction with the desired analyte.

### Functionalization using oligonucleotides

Oligonucleotides are poly-nucleic acid chains made up from nitrogen-containing bases, five-carbon sugars, and phosphate groups. The monomers of oligos are adenosine (A), guanosine (G), cytidine (C), thymine (T), and uridine (U). The

incorporation of specific ligands (such as thiol or amine modifications) at the 5'- or 3'-terminal of oligonucleotides enables the interaction of oligos with plasmonic nanoparticles. The easy synthesis process and the programmable assembly of oligonucleotides make them an ideal functionalization agent for NPs.

Zhu and co-workers [57] have proposed a facile Cr<sup>3+</sup> and adenosine determination using the aptamer and 11-mercaptoundecanoic acid assembled gold nanoparticles. The detection limit of mentioned target is calculated to be  $1.7 \times 10^{-11}$  M and  $1.8 \times 10^{-8}$  M, respectively. The thiolated DNA and 11-mercaptoundecanoic acid (MUA) was simultaneously assembled to the surface of gold nanoparticles in one step by gold-sulfur interaction. The principle of detection was that Cr<sup>3+</sup> bind preferentially with -COOH group in the structure of MUA through the chelation interaction. As a result, the interparticle distance of AuNPs was greatly decreased in the presence of Cr<sup>3+</sup>, causing a red shift of the SPR peak and a visual color change from red to blue. Busayapongchai and Siri [58] developed a sensitive determination method for estradiol (E2) based on plasmonic properties of gold nanoparticles. This developed assay exhibited a wide dynamic range from  $10^{-15}$  to  $10^{-8}$  M for E2 determination. The mechanism of detection is based on the ligand binding domain of estrogen receptors (LBD-ER $\alpha$ ) and gold nanoparticles using pre-designed DNA aptamers. Jia et al. [59] have proposed a colorimetric sensing assay based on exonuclease I-triggered aggregation of DNA-functionalized gold nanoparticles for discriminations of different proteins. This sensor was able to discriminate 15 proteins with a detection limit of 10 nM in buffer solution and real serum samples. The oligonucleotides were immobilized on AuNP surfaces through the Au-S bond. Chu and colleagues [60] have introduced a facile method for the determination of mercury based on AuNPs and mercury-specific-oligonucleotide-conjugated resonators (MSOIRs) with a detection limit of 100 pM. The functionalization process of AuNPs is based on the binding of activated thiol groups at the end of DNAs and AuNPs surface (Fig. 4(a)). In another study, an optical biosensor was developed for the simultaneous detection of a variety of *Salmonella spp.* in environmental and food samples via oligonucleotide-functionalized gold nanoparticles [46]. This colorimetric sensor has a detection limit of < 10 CFU/mL for both pure culture and complex matrix setups. Highly specific oligonucleotides were designed and conjugated onto the surface of AuNPs via thiol linkage, HS-(CH<sub>2</sub>)<sub>6</sub>, which was initially introduced chemically to either 5'- or 3'- end of the oligonucleotide probes. Figure 4(b) shows the sensing strategy for positive and negative response for sensitive determination of *Salmonella spp.* using AuNPs.

Zou and colleagues [62] have constructed a novel colorimetric sensing assay for biomolecule detection which integrates the signal amplification of hybridization chain reaction

**Table 1** Summary of previous efforts for functionalization of plasmonic nanostructures using proteins and amino acids for sensing purposes

Analyte	Functional ligand/moiety	Limit of detection (LOD)	References
Hg <sup>2+</sup>	L-Cysteine/NM*	10 <sup>-8</sup> M	[41]
Hg <sup>2+</sup>	Glutamine and histidine/carboxylic and amino groups	0.90 μM	[43]
Ci <sup>3+</sup> , Pb <sup>2+</sup>	Tyrosine/NM	1, 2 μM	[42]
Copper ion	Tyrosine/phenolic and hydroxyl groups	150 nM	[45]
Glutathione	Ascorbic acid/multi-donate anchoring groups (SH, -NH <sub>2</sub> , -COO <sup>-</sup> )	2.4 × 10 <sup>-7</sup> M	[46]
Mg <sup>2+</sup>	Tryptophan/NM	0.2 μM	[56]
Atrazine	N-methacryloyl L-aspartic acid (MAAsp)/NM	0.7134 ng/mL	[54]
Hg <sup>2+</sup>	Gelatin/amalgam (Hg-Ag)	25 nM	[39]
Cu <sup>2+</sup> , Fe <sup>3+</sup>	Glutathione/NM	0.125, 1.25 nM	[40]
Carcinoembryonic antigen (CEA)	Peptide/NM	NM	[44]
Bacterial pathogens	Cysteine modified synthetic antimicrobial peptides (sAMPs)/peptide bonding (S-Au)	10 <sup>2</sup> CFU/mL	[52]
hlgG	Human immunoglobulin G antibody (anti-hlgG)/NM	11 ng mL <sup>-1</sup>	[47]
IFX and ATI	TNFα	2.5 μg/mL	[48]
Tetracycline (TC)	Mercaptoundecanoic acid (MUA) and antibody pair (anti (TC))/NM	10 aM	[50]
Alpha-1 antitrypsin (AAT) and Tau 381	Mixed antibody (anti-AAT and anti-Tau)/NM	μM and fM scale	[51]
C-reactive protein (CRP)	Aptamer antibody/3'-thiol-modified 6th-62-40	10 pM	[53]
Diphtheria toxin (DT)	Monoclonal anti-diphtheria IgG/NM	10 ng/mL	[55]

\*NM = not mentioned

(HCR) with the assembly of gold nanoparticles through triplex formation with the detection limit of 5 pM, 10 pM, 5 nM, and 20 pM for DNAs, microRNAs, ATPs, and PDGF-BBs, respectively. DNA hairpin probes can form rigid triplex structures with triplex-forming oligonucleotide (TFO)-functionalized AuNPs in the absence of targets, which will aggregate in the presence of biomolecule targets. The reviewed literatures are summarized in Table 2.

When the sensitivity of the sensor is the ultimate goal, oligonucleotide functionalization is the best choice. Due to the specific interactions with the desired analyte, high selectivity could be obtained with the LOD usually lower than nM concentrations. Even though the oligonucleotides for specific analytes are well known, a time- and cost-consuming process should take over if the specific oligonucleotide is unknown for the desired analyte. On the other hand, the assembly of oligonucleotide on the NP surface is not a tough job and can be realized using amine or thiol modification in the oligos.

### Functionalization using polymers

Polymer-functionalized nanostructures are known for their ability to create the desired surface functionalities. Both

synthetic and organic polymer-functionalized NPs are widely used for biosensing because of their non-toxic and non-immunogenic properties [63–65]. Maruthupandy and colleagues [66] proposed a simple method for the rapid colorimetric and visual detection of glucose molecules in water medium with a linear range from 5 to 100 μM using chitosan capped-AgNPs (CS/AgNPs). Silver nanoparticles were interacted with the O<sub>2</sub> from hydroxyl group in chitosan as well confirmed with FTIR spectroscopy. The interaction of glucose molecules with CS/AgNPs decreased the interparticle distance significantly. The spectral relation as well as visual change upon the addition of glucose is shown in Fig. 5.

Also, a rapid and simple colorimetric method based on the surface plasmon resonance of polyvinylpyrrolidone (PVP)-stabilized AgNPs was developed for the detection of the Timolol (a cardiovascular drug) by Amirjani et al. [67] with the LOD of 1.2 × 10<sup>-6</sup> M. Based on the proposed mechanism, the chemisorption of the Timolol drug on the AgNPs via Ag-S binding induces the aggregation of AgNPs.

In another study, a localized surface plasmon resonance sensor based on gold nanorods functionalized with polyethylene glycol was developed for the determination of activated leukocyte cell adhesion molecule (ALCAM) cancer

**Fig. 4** (A) Schematic illustration of mercury ion detection using resonance frequency shift of a MSOIR on AuNPs surface. Reproduced with permission from reference [44]. (B) (a) Sensing strategy for colorimetric detection of *Salmonella spp.* using optical properties of aggregated versus non-aggregated AuNPs. The TEM images in (b) and (c) show the absence and presence of analyte in the solution, respectively. Reproduced with permission from reference [61]

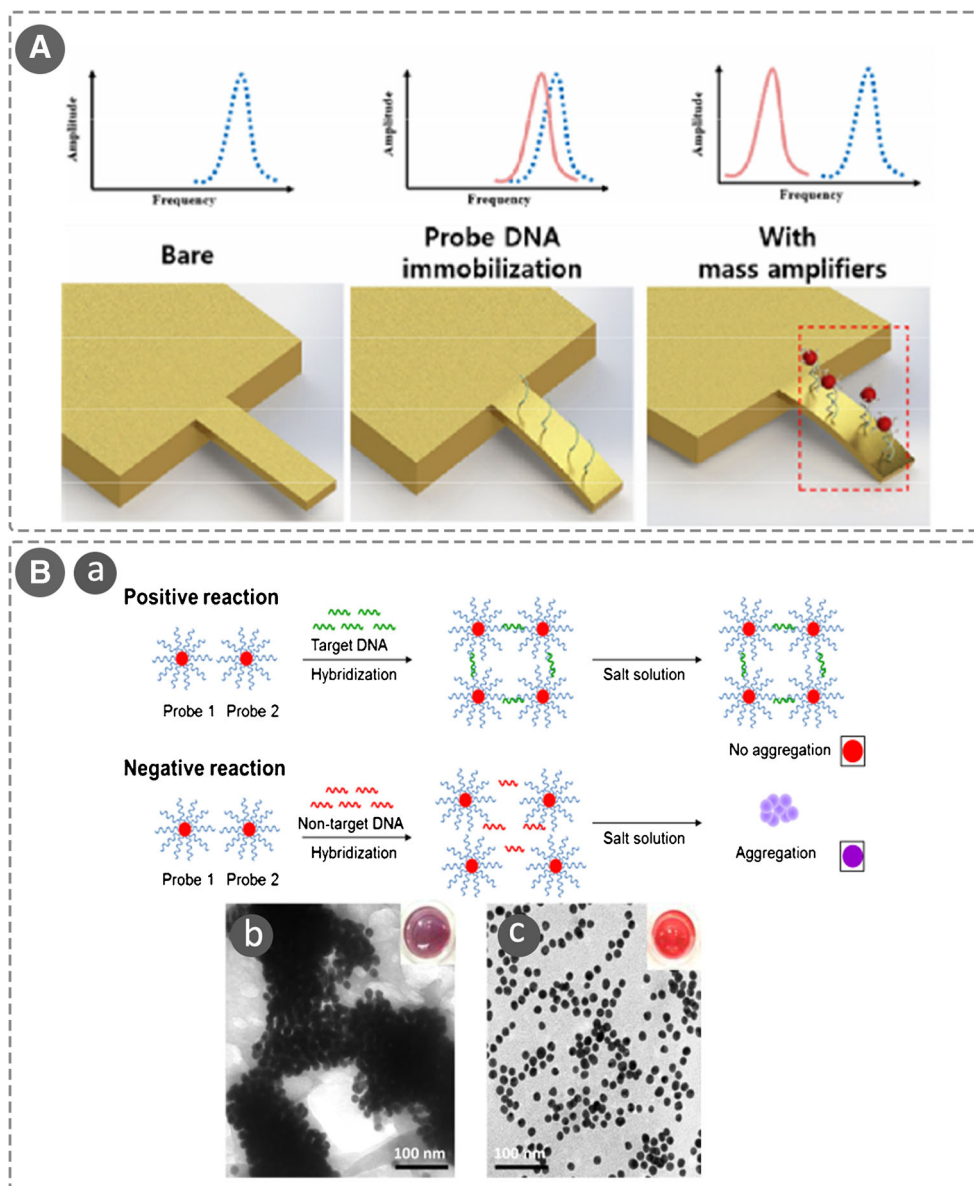


**Table 2** Summary of previous efforts for functionalization of plasmonic nanostructures using oligonucleotides for sensing purposes

Analyte	Functional ligand/moiety	Limit of detection (LOD)	Reference
Cr <sup>3+</sup> , Adenosine	Aptamer and 11-mercaptoundecanoic acid / -COOH	1.7 × 10 <sup>-11</sup> M and 1.8 × 10 <sup>-8</sup> M	[57]
Estradiol (E2)	Estrogen receptorα (LBD-Era)/specific interaction	2.62 × 10 <sup>-14</sup> M	[58]
15 different proteins	DNA sequence/NM*	10 nM	[59]
Mercury	Mercury-specific-oligonucleotide-conjugated resonators (MSOIRs)/NM	100 pM	[60]
Variety of <i>Salmonella spp.</i>	Specific oligonucleotides/NM	<10 CFU/mL	[61]
DNA, microRNAs, ATPs, PDGF-BBs	Specific oligonucleotides/NM	5 pM, 10 pM, 5 nM, 20 pM	[62]

\*NM = not mentioned

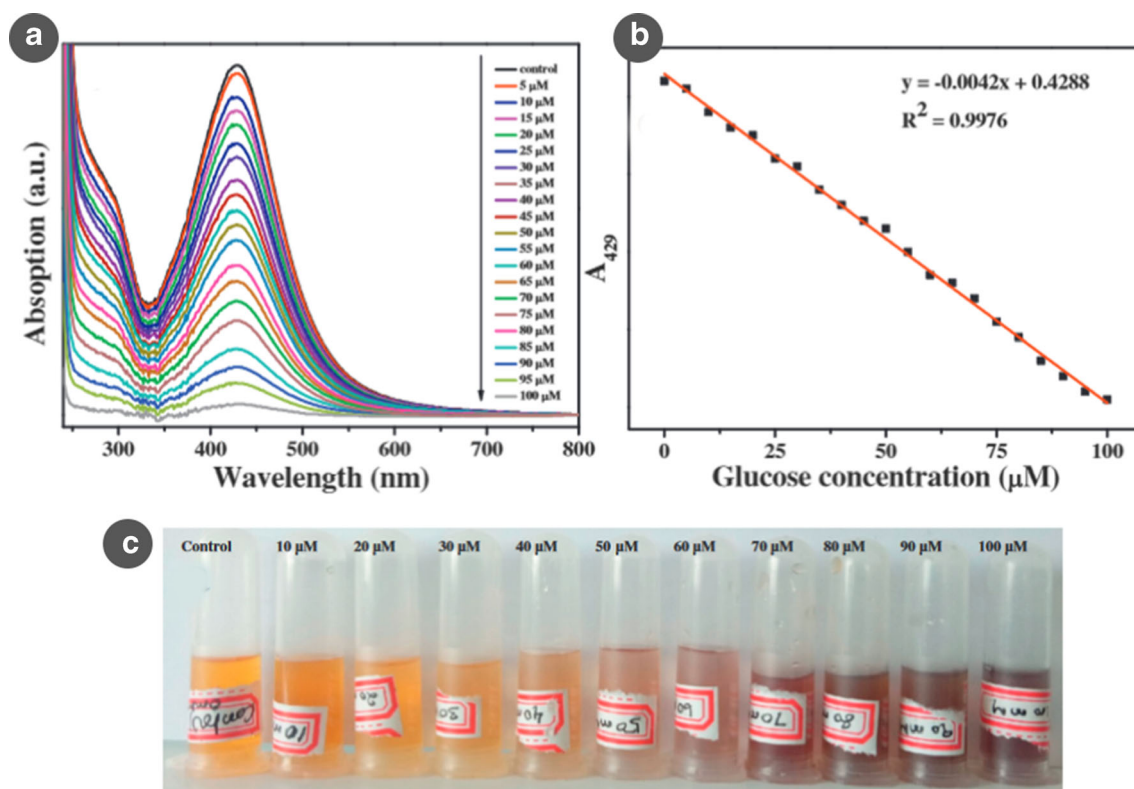


**Fig. 5** (a) and (b) show the relationship between absorbance at 429 nm and the concentration of glucose in the solution in the range of 5–100  $\mu\text{M}$ . (c) shows the visual color change in the presence of different glucose concentrations. Reproduced with permission from reference [66]

biomarker [53]. Both high- and low-molecular weight thiolated PEG molecules were used to provide effective steric hindrance as well as ample reactive groups for conjugation with the biomolecular probes. This strategy leads to increased sensitivity of the developed sensor and allowed the detection of the ALCAM antigen concentration down to 15  $\mu\text{M}$ . A sensitive and selective  $\text{Hg}^{2+}$  optical sensor has been developed based on the redox interaction of  $\text{Hg}^{2+}$  with starch-coated silver nanoparticles in the presence of  $0.005 \text{ molL}^{-1} \text{ HNO}_3$  by Vasileva and coworkers [68] with the detection limit of  $0.9 \mu\text{gL}^{-1}$ . The formation of Ag-Hg amalgam due to the sorption and reduction of positively charged  $\text{Hg}^{2+}$  on the surface of negatively charged AgNPs was known as the responsible mechanism of this sensor (Fig. 6).

Buccolieri et al. [69] have developed a colorimetric sensor for ammonia sensing in aqueous solutions based on bio-synthesized AgNPs using sucralose and glucose. The mentioned sensor could detect ammonia in the range of  $10^{-2}$  to  $10^3$  ppm in aqueous solutions. In another study, Ban and colleagues [70] have developed a spectroscopy based method for sensing  $\text{Hg}^{2+}$  and cellular-free oxygen radical via starch-functionalized silver nanoparticles. Starch was used as the reducing agent as well as capping agent, and NaOH played the role of a catalyst for converting  $\text{AgNO}_3$  to  $\text{AgO}_2$  and Ag, respectively. It was observed that starch-functionalized AgNPs were highly sensitive to  $\text{Hg}^{2+}$  ions as reflected from

the blue shift in the absorption spectra. In the presence of  $\text{Hg}^{2+}$ , the interaction between silver and mercury forms amalgam. Li et al. [71] have presented a paper-based colorimetric sensor using  $-\text{NH}_2$  and  $-\text{SH}$  decorated AuNPs for rapid determination of  $\text{Fe}^{3+}$  ions. The leaching of gold nanoparticles in the presence of thiourea or hydrogen peroxide can speed up by using catalytic  $\text{Fe}^{3+}$  ions, and this method is capable to detect ferric ions as low as  $0.85 \mu\text{M}$ . In another study, poly(allylamine hydrochloride) (PAH) and poly(sodium 4-styrenesulfonate) (PSS) were used to functionalize gold nanoparticles for colorimetric determination of  $\text{Hg}^{2+}$  and  $\text{Cd}^{2+}$  in water samples [58]. Two bi-layers of polyelectrolytes were deposited on the AuNP-functionalized sensor probes for giving a better RI sensitivity (down to 0.5 ppb) compared with single bi-layer. In another study, a rapid and straightforward method was developed for colorimetric determination of ammonia using smartphones based on PVP-stabilized AgNPs [59]. In order to evaluate the effect of ammonia on the UV-vis spectrum of the synthesized silver nanoparticles, different levels of ammonia (in the range of 10–1000  $\text{mg L}^{-1}$ ) were added to the colloidal solution of AgNPs containing a constant level of the nanoparticles. The mechanism of the detection is based on the formation of a complex ( $\text{Ag}(\text{NH}_3)_2^+$ ) which is accompanied by the decrease in the number of individual AgNPs and their related characteristics surface plasmon band. The main point of this study was the use of a smartphone for



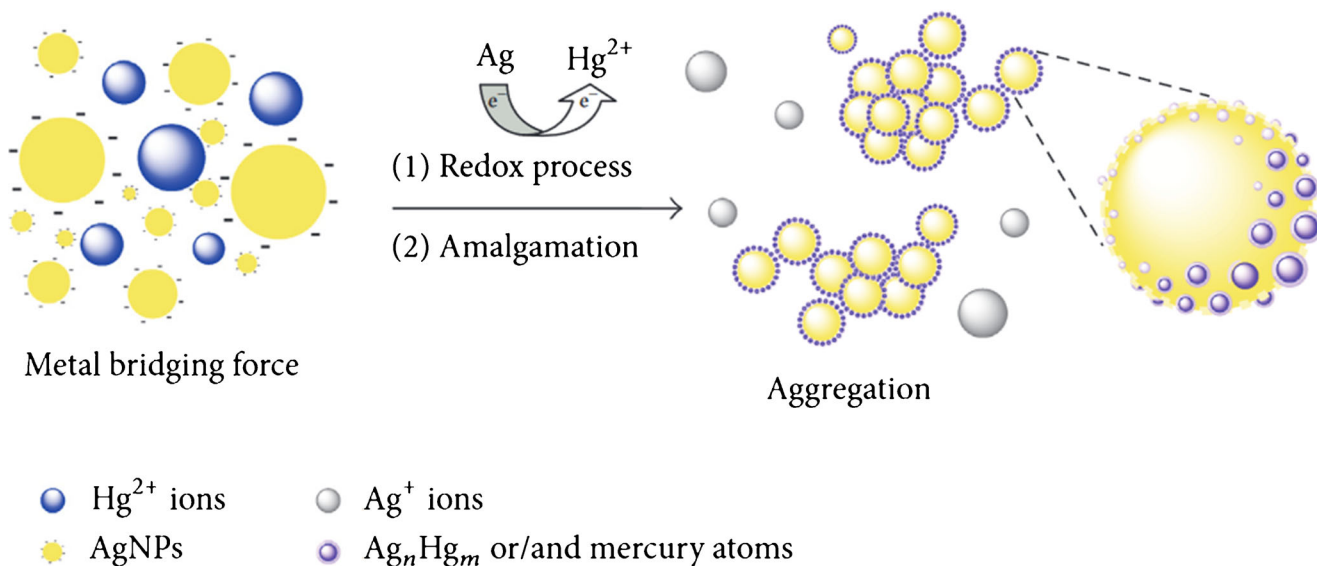


**Fig. 6** The amalgamation process by interaction of  $\text{Hg}^{2+}$  ions with negatively charged silver nanoparticles. Reproduced with permission from reference [68]

colorimetric measurements instead of a UV-Vis spectrophotometer. The smartphone-based detection has the capability to detect ammonia with the LOD as low as 200 ppm. Acrylamide, cellulose, sodium alginate, and sodium cholate were also used in previous literatures for functionalization of nanoparticles [72–76]. Table 3 presents a complete list of polymers for functionalization with responsible moiety in their structure.

The main advantage of polymers as functional agents is their ability to host different moieties with a simple polymerization reaction. The bonding to NPs can be realized using amine or thiol modification as well as the desired moiety for analytical process, which can be grafted in the structure of polymers. However, most of the works in this field are based on non-specific interaction of polymers with NPs and the analytes, which will not yield extremely low detection limits.

### Functionalization using organic compounds

Functionalization of plasmonic nanoparticles using organic compounds is the mostly endeavored mechanism for designing colorimetric sensors. The main reason is the diversity of chemical compounds and the ability to design the required surface chemistry for selective determination of specific analyte. The main strategy for linking to metal NPs is via S-H and  $\text{NH}_3$  linkage and several chemical moieties (e.g., hydroxyl, carboxyl, carbonyl, etc.) can be available as an anchor to the analytes.

For instance, a simple colorimetric citrate-capped silver nanoparticle-based sensor have been proposed by Zheng et al. [80] for the determination of thiophanate-methyl (TM) in the range of 2–100  $\mu\text{M}$  with a detection limit of 0.12  $\mu\text{M}$ . Their approach is based on the color change of cit-AgNPs from yellow to cherry red with the addition of TM to Cit-

AgNPs that caused a redshift on the SPR band from 394 to 525 nm due to the hydrogen-bonding and substitution. The absorbed citrate ions on the surface of AgNPs are capable of forming the hydrogen bonding with thiophanate-methyl through  $-\text{COOH}$  group of citrate and  $-\text{NH}$ ,  $-\text{C}=\text{S}$ ,  $-\text{C}=\text{O}$ ,  $-\text{CH}_3$  groups of thiophanate-methyl. In another study, a colorimetric sensor based on sulfoanthranilic acid dithiocarbamate (SAA-DTC)-functionalized AgNPs was developed by Mehta and colleagues [81] for the detection of  $\text{Mn}^{2+}$  and  $\text{Cd}^{2+}$ , with the detection limit of 1.7 and 5.7  $\mu\text{M}$ , respectively. Disappearing of stretching and bending modes of S-H group indicates the successful attachment of SAA-DTC on the surface of AgNP via thiolate linkage. Sensing mechanism of the above-mentioned sensor is based on the aggregation of SAA-DTC AgNPs in the presence of  $\text{Mn}^{2+}$  and  $\text{Cd}^{2+}$ . In another study, a sensitive and low-cost colorimetric probe was developed by introducing a linkage between 1-amino-2-naphthol-4-sulfonate (ANS) and triangular silver nanoplates by electrostatic interaction of the sulfo groups, for  $\text{Cd}^{2+}$  sensing in narrow linear range of 30–70  $\mu\text{M}$  with a limit of detection of 30 nM [67]. ANS can bind to  $\text{Cd}^{2+}$  ions through  $\text{NH}_2$ ,  $\text{SO}_3$ , and OH groups, which leads to the aggregation of triangular AgNPs. Song and colleagues [82] have developed a low-cost, rapid, simple, and sensitive assay using sulfanilic acid-functionalized silver nanoparticles (SAA-AgNPs) for melamine detection in pretreated milk samples, with a LOD of 10.6 nM. In the presence of melamine, the SAA-AgNPs aggregated rapidly through hydrogen bonding between  $-\text{NH}_2$  groups on the outer surface of the SAA and the melamine molecule. Surface modification of AgNPs was done by Neem Gum (NG), containing complex polysaccharides, proteins, and other organic compounds, as the reducing and stabilizing agent [69]. FTIR analysis has demonstrated the

**Table 3** Summary of previous efforts for functionalization of plasmonic nanostructures using polymers for sensing purposes

Analyte	Functional ligand/moiety	Limit of detection (LOD)	Reference
Glucose	Chitosan/NM*	5 $\mu\text{M}$	[66]
Timolol	Polyvinylpyrrolidone (PVP)/-SH	$1.2 \times 10^{-6}$ M	[67]
Activated leukocyte cell adhesion molecule (ALCAM) cancer biomarker	Polyethylene glycol/NM	15 pM	[77]
Hg <sup>2+</sup>	Starch/NM	0.9 $\mu\text{gL}^{-1}$ (in range of 0–12.5 $\mu\text{gL}^{-1}$ ) 2.7 $\mu\text{gL}^{-1}$ (in range of 25–500 $\mu\text{gL}^{-1}$ )	[68]
Ammonia	Surcralose and Glucose/NM	$10^{-2}$ – $10^{-3}$ ppm	[69]
Hg <sup>2+</sup> & cellular free oxygen radical	Starch/NM	NM	[70]
Fe <sup>3+</sup>	-NH <sub>2</sub> , -SH	0.85 $\mu\text{M}$	[71]
Hg <sup>2+</sup> , Cd <sup>2+</sup>	Poly(allylamine hydrochloride) (PAH) and Poly(sodium 4-styrenesulfonate) (PSS)/NM	0.5 ppb	[78]
Ammonia	Polyvinylpyrrolidone (PVP)/NM	200 ppm	[79]
Ag <sup>+</sup>	Hyperbranched polyethylenimine (HPEI)/-SH	$8.76 \times 10^{-8}$ M (naked eye) $8.76 \times 10^{-9}$ M (UV-Vis)	[73]
Acrylamide	Acrylamide/C=C	0.2 nM	[72]
H <sub>2</sub> O <sub>2</sub>	Polysaccharide (cellulose nanowhiskers)/NM	0.014 $\mu\text{M}$ (in range of 0.1–30 $\mu\text{M}$ ) 112 $\mu\text{M}$ (in range of 60–600 $\mu\text{M}$ )	[74]
Hg <sup>2+</sup>	Sodium alginate/NM	5.29 nM	[75]
Hg <sup>2+</sup> , Pb <sup>2+</sup>	Sodium Cholate/COO <sup>-</sup> and -OH	12 nM, 60 nM	[76]

\*NM = not mentioned

binding of hydroxyl, carbonyl, carboxyl, and amine groups of amino acid and NG proteins to the surface of AgNPs. In another study, 2-Mercaptoethanesulfonate (MES) was used to develop a selective and sensitive sensor for alkaline and alkaline earth metal cation determination and monitoring in biological samples [70]. Their SERS-based sensor exhibits limits of detection of 10 nM for Ca<sup>2+</sup> and 1  $\mu\text{M}$  for Co<sup>2+</sup>, Fe<sup>2+</sup>, and Mn<sup>2+</sup> with a mechanism based on attractive interaction between negative charges of MES attached to the surface of AgNPs and cations present in the solution. Patel and colleagues [83] have developed a simple, rapid, and sensitive colorimetric method for the determination of carbendazim using 4-aminobenzenethiol-functionalized silver nanoparticles (ABT-AgNPs) as a colorimetric sensor. Under optimum conditions, the absorbance ratio at A<sub>510</sub>/A<sub>397</sub> is linearly related to the concentration of carbendazim in the range of 10–100  $\mu\text{M}$ , with a detection limit of 1.04  $\mu\text{M}$ . This colorimetric method has been successfully utilized to detect carbendazim in environmental water and food samples. Since ABT-AgNP surface exhibits positive charges (pKa of ABT is 5.70) whereas carbendazim bears negative charges (pKa is 4.48), the conjugation of carbendazim with ABT-AgNPs results to aggregation of NPs via strong ion-pair interactions. The  $\pi$ - $\pi$  interactions between the neighboring carbendazim-conjugated ABT-AgNPs are responsible for the aggregation that result a

color change from yellow to orange and a red-shift in SPR band of ABT-AgNPs from 397 to 510 nm. The formation of a new bond between ABT and AgNPs was approved by disappearance of -SH group located at 2543–2550 and 935–945  $\text{cm}^{-1}$ .

In another research by Devadiga and colleagues [84], aqueous extract of an agrowaste: *Terminalia catappa* leaves was used to reduce and functionalize AgNPs with possible application for Hg<sup>2+</sup> sensing. Authors believed that the multifunctional groups (e.g., hydroxyl, carboxyl, and heteroaromatic rings) present in the extract are responsible for interaction with mercury ion and enhanced stability of the nanoparticles. There are also other reports on using biosynthesized nanoparticles as optical sensors for Hg<sup>2+</sup>, Cr<sup>6+</sup>, Zn<sup>2+</sup>, and hydrogen peroxide determination [85–87]. Silver triangular nanoplates conjugated with gallic acid were designed as a probe for colorimetric detection of reduced GSH with a limit of detection of 0.12 nM [76]. The functionalization of nanoplates was easily done through the phenolic hydroxyl groups (-OH) of gallic acid. The authors believed that the interaction of deprotonated carboxylate (COO<sup>-</sup>) of gallic acid with protonated amine (NH<sub>3</sub><sup>+</sup>) is responsible for aggregation of nanostructures. Muthivhi et al. [88] have developed a green method for sensing Hg<sup>2+</sup> in aqueous media via gelatin-noble metal polymer nanocomposites with a detection limit of

$10^{-3}$  nM. The interaction of gelatin with AgNPs was done via coordination with nitrogen from the amide group.

Silver nanoparticles capped with 3-mercaptopropanesulfonic acid (AgNPs-3MPS) were used to develop a colorimetric sensor for  $\text{Ni}^{2+}$  or  $\text{Co}^{2+}$  ions in water based on the change of the intensity and shape of SPR peak [78]. The reported sensor has a good sensitivity for the detection of  $\text{Ni}^{2+}$  or  $\text{Co}^{2+}$  ions in aqueous solutions up to 500 ppb. The interaction of MPS with AgNPs was done via thiol-linkage. Pinyorospatum and co-workers [89] have presented a sensitive colorimetric sensor for the determination of phosphate ions ( $\text{P}_i$ ) performed on paper-based analytical devices (PADs) based on the anti-aggregation of 2-mercaptoethanesulfonate (MS)-modified silver nanoplates. This sensor has a detection limit of  $0.33 \text{ mg L}^{-1}$  and a limit of quantification equal to  $1.01 \text{ mg L}^{-1}$  for determination of phosphate ions in the range of  $1\text{--}30 \text{ mg L}^{-1}$ . The presence of -C-H, -COO-, or -COOH stretching modes in FTIR spectra proved the assembly of 2-mercaptoethanesulfonate on AgNPs surface. In addition, the absence of thiol band (-S-H) at  $2550 \text{ cm}^{-1}$  can be attributed to the formation of Ag-S bonds. Chen and colleagues [90] have introduced an adrenaline sensor based on 4-amino-3-hydrazino-5-mercapto-1,2,4-triazol (AHMT)-functionalized gold nanoparticles with a wide linear range of  $7 \text{ nM}\text{--}0.1 \text{ mM}$  and the detection limit of  $1 \text{ nM}$ . Sensing mechanism is based on aggregation of AuNPs which was specially induced by the binding of AHMT to adrenaline as a result of hydrogen bonding between the two molecules, leading to a color change from wine-red to purple-blue. Adrenaline molecule has one amine group and three hydroxyl groups. Each adrenaline molecule has four sites to form hydrogen bonds of NH-O and NH-N. Thus, the aggregation of AHMT-AuNPs was induced by hydrogen bonding between the AHMT and adrenaline. Organically functionalized gold nanoparticles were developed as a prototype gas sensor for formaldehyde detection with possible applications in non-invasive diagnosis through exhaled breath analysis [81]. In this study, 2-mercaptobenzoxazole ( $\text{C}_7\text{H}_5\text{NOS}$ ) was used to functionalize the AuNPs. A colorimetric method for the detection of  $\text{Fe}^{3+}$  in water and biological samples is introduced via oxamic acid (OA) and p-aminobenzoic acid (PABA) functionalized gold nanoparticles (OA-PABA-Au NPs) as a probe [82]. This sensor exhibits a detection limit of  $5.83 \text{ }\mu\text{M}$ . According to the FTIR measurements, OA and PABA molecules were successfully assembled on the surfaces of AuNPs via Au-N linkage. The addition of  $\text{Fe}^{3+}$  ion leads to a decrease in the SPR band intensity of OA-PABA-AuNPs at  $523 \text{ nm}$  and to generate a new SPR peak at  $685 \text{ nm}$ , confirming that the aggregation of OA-PABA-AuNPs induced by  $\text{Fe}^{3+}$  ion, which results a color change from red to blue. Khodaveisi and colleagues [91] have proposed a colorimetric sensor for the determination of naproxen (NAP) based on the aggregation of the thiolated  $\beta$ -cyclodextrin ( $\text{T}\beta\text{-CD}$ )-functionalized gold nanoparticles ( $\text{T}\beta\text{-CD-AuNPs}$ ) in the presence of NAP and  $\text{Zn}^{2+}$  with a detection limit of  $0.6 \text{ }\mu\text{g L}^{-1}$  in the range of  $4\text{--}180 \text{ }\mu\text{g L}^{-1}$ . It is known that NAP can act as a unidentate ligand

through its carboxylate group and form complexes with several transition metal ions while the other end of NAP is hydrophobic and has high affinity to interact with molecules such as CD. Furthermore, due to the hard and soft acid-base interaction, the thiolated molecules have the ability to interact with the surface of AuNPs and displace the shell of citrate groups. The  $\beta$ -CD was thiolated and immobilized on the surface of synthesized AuNPs. Then,  $\text{Zn}^{2+}$  which forms a colorless complex with NAP was selected as transition metal ions and along with NAP was added to the  $\text{T}\beta\text{-CD-AuNP}$  solution. This resulted in the formation of  $(\text{T}\beta\text{-CD:NAP})_2\text{Zn}$  complex through aggregation of AuNPs, and because of the near-field coupling in the resonant wavelength peak of the interacting particles, the original LSPR peak of AuNPs decreases, and a new red-shifted band at  $650 \text{ nm}$  appears. Qin et al. [92] have employed AHMT-AuNP for sensitive determination of kanamycin (KA) in the range of  $0.005\text{--}0.1 \text{ }\mu\text{M}$  and  $0.1\text{--}20 \text{ }\mu\text{M}$  with a limit of detection of  $0.004 \text{ }\mu\text{M}$ . AHMT contains one mercapto group, which can strongly coordinate to the surface of AuNPs. In addition, AHMT has two exocyclic amino groups and a three nitrogen hybrid ring. On the other hand, as an aminoglycoside antibiotic, KA has four amino groups ( $-\text{NH}_2$ ) and seven hydroxyl groups ( $-\text{OH}$ ) which may combine with the AHMT through hydrogen-bonding interaction. The aggregation of AHMT-AuNPs in the presence of KA was studied by monitoring the shift of SPR band.

Khodaveisi and co-workers [93] have reported a colorimetric sensor based on the aggregation of the  $\text{T}\beta\text{-CD}$  functionalized gold nanoparticles for the determination of nabumetone (NAB) in the presence of PVP with a LOD of  $0.2 \text{ }\mu\text{g L}^{-1}$ . In this study, PVP has the key role to increase the affinity of  $\beta$ -CD for NAB. Formation of the ternary complex of  $\text{NAB}:(\beta\text{-CD})_2\text{-PVP}$  resulted in the aggregation of NPs.

Chen and colleagues [94] have synthesized Rhodanine-stabilized gold nanoparticles in order to construct a colorimetric sensor for selective determination of  $\text{Hg}^{2+}$  in the range of  $0.02\text{--}0.5 \text{ }\mu\text{M}$ . The detection limit of this sensor was measured to be  $6.0 \text{ nM}$ . The assembly of Rhodanine on AuNPs was done via thiol sub-unit molecules through gold-thiol (Au-S) affinity interactions. Upon the addition of  $\text{Hg}^{2+}$  to AuNPs@R, a new absorption band at  $650 \text{ nm}$  appeared and dispersed AuNPs@R are induced to aggregate via the formation of the  $\text{R-Hg}^{2+}\text{-R}$  structure. A sensitive biosensor based on functionalized nanoporous gold (NPG) has been constructed for the determination of human serum albumin (HSA) [95]. In order to study the Raman signal produced by modified NPG substrates, four different compounds (i.e., cysteamine, 3-mercaptopropionic acid, 4-aminothiophenol, 4-mercaptobenzoic acid), all provided with a sulfidric group to be bound to the gold surface, were tested after their immobilization on nanostructured gold surface of given porosity. The structural differences among the selected molecules concern the functional group (i.e., amino or carboxyl) used to link covalently to the antibody and the aliphatic or aromatic nature of the structure themselves. All these molecules are bifunctional with a thiol

**Table 4** Summary of previous efforts for functionalization of plasmonic nanostructures using organic compounds for sensing purposes

Analyte	Functional ligand/moiety	Limit of detection (LOD)	Reference
Hg <sup>2+</sup>	Citrate/amalgam (Hg-Ag)	4 nM	[5]
Thiophanate-methyl (TM)	Citrate/hydrogen bonding	0.12 μM	[80]
Mn <sup>2+</sup> , Cd <sup>2+</sup>	Sulfonathranilic acid dithio carbamate (SAA-DTC)/NM	1.7, 5.7 μM	[81]
Cd <sup>2+</sup>	1-amino-2-naphthol-4-sulfonate (ANS)/NH <sub>2</sub> , SO <sub>3</sub> , OH	30 nM	[97]
Melamine	Sulfonic acid (SAA)-NH <sub>2</sub>	10.6 nM	[82]
Ca <sup>2+</sup> , Co <sup>2+</sup> , Fe <sup>2+</sup> , Mn <sup>2+</sup>	2-Mercaptoethanesulfonate (MES)/NM*	10 nM, 1 μM, 1 μM, 1 μM	[98]
Carbendazim	4- aminobenzenethiol/NM	1.04 μM	[83]
Hg <sup>2+</sup>	Extract of <i>Terminalia catappa</i> leaves/NM	NM	[84]
Hydrogen peroxide	Kiwifruit extract/NM	5.0 × 10 <sup>-7</sup> M	[85]
Cr <sup>6+</sup> , Ammonia	Durenta erecta ( <i>D. erecta</i> )/metal-oxygen bonding	Up to 0.1 ppm	[86]
Hg <sup>2+</sup>	<i>Matricaria recutita</i> (Babunah) plant extract / NM	100 ppm	[87]
Reduced glutathione (GSH)	Gallic Acid/NM	0.12 nM	[99]
Hg <sup>2+</sup>	Gelatin/NM	10 <sup>-3</sup> nM	[88]
Ni <sup>2+</sup> , Co <sup>2+</sup>	3-mercapto-1 propanesulfonic acid (3MPS)/NM	500 ppb	[100]
Phosphate ion	2-mercaptoethanesulfonate (MS)/NM	NM	[89]
Adrenaline	4-amino-3-hydrazino-5-mercapto-1,2,4-triazol (AHMT)/NM	1 nM	[90]
formaldehyde	2-mercaptobenzoxazole (C <sub>7</sub> H <sub>5</sub> NOS)/NM	NM	[101]
Fe <sup>3+</sup>	Paminobenzoic acid (PABA), Oxamic acid (OA) / NM	5.83 μM	[102]
Naproxen (NAP)	Thiolated β-cyclodextrin (Tβ-CD) and Zn <sup>2+</sup> /carboxylate group	0.6 μg L <sup>-1</sup>	[91]
Kanamycin (KA)	4-amino-3-hydrazino-5-mercapto-1,2,4-triazole (AHMT)/amine and hydroxyl groups and hydrogen bonding		[92]
Nabumetone (NAB)	Thiolated β-cyclodextrin (Tβ-CD) / NM	0.2 μg L <sup>-1</sup>	[93]
Hg <sup>2+</sup>	Rhodanine/NM	6.0 nM	[94]
Human serum albumin (HSA)	Cysteamine, 3-mercaptopropionic acid, 4-aminothiophenol, 4-mercaptobenzoic acid/amine or carboxyl (amide bond with antibody)	NM	[95]
Pencycuron fungicide	6-aza-2-thiothymine (ATT)/NM	0.42 μM	[96]
Dopamine (DA)	S-doped carbon dots (S-CD)/carboxylic group of CDs and amine groups of DA	0.23 μM	[103]
HER2-positive breast cancer cell (SKBR3)	Liposome/anti-HER2	5 single cells	[104]
Cu <sup>2+</sup>	1,3-alternate calix[4]arene/NM	2.5 × 10 <sup>-6</sup> M	[105]
Hg <sup>2+</sup>	Mercaptobenzoheterocyclic compounds (MBO, MBI, MBT)/Ag-Hg interaction	9.2 pM (MBO) 46 pM (MBI) 92 pM (MBT)	[106]
As <sup>3+</sup>	Polyethylene glycol (PEG) / - OH	1 ppb	[107]
Hg, Hg <sup>+</sup>	Calixarene / Ag-Hg interaction	0.5 nM (UV-Vis) 10 nM (Amperometry)	[108]

\*NM = not mentioned

group able to form the Au-S bond to NPG and an amino or carboxylic terminal group that gives an amide bond with the antibody. Aromatic moieties have been preferred to aliphatic ones due to a more oriented interaction of the molecule with the NPG surface, while the choice between the two aromatic moieties (i.e., 4ATP and 4MBA) has been affected by the strategy used to generate the amide bond with the antibody.

Kailasa and colleagues [96] have proposed a facile method for developing a colorimetric sensor based on the pencycuron-induced aggregation of 6-aza-2-thiothymine (ATT)-functionalized gold nanoparticles for the determination of pencycuron fungicide in rice, potato, cabbage, and water samples with the detection limit of 0.42 μM in the range of 2.5–100 μM. ATT can easily displace citrate molecules on the surfaces of AuNPs



and tune the visual readout ability of AuNPs towards a specific analyte. ATT contains a mercapto group that can easily form a covalent bond (via Au-S bond) with the surface of AuNP. In another study, a selective colorimetric sensor has been proposed based on LSPR of S-doped carbon dots-functionalized gold nanoparticles for detection of dopamine (DA) with a detection limit of 0.23  $\mu\text{M}$  [89]. In this study, phenylamine-4-sulfonic acid with abundant thiol functional groups interacted with Au NPs through soft-soft acid-base interaction. It was observed that addition of DA molecules followed by  $\text{Fe}^{3+}$  causes aggregation of DA-S-CDs@Au NPs resulting in a decrease in the LSPR band of modified AuNPs around 520 nm and the appearance of a new band at 670 nm. This observation is due to the assembly of DA molecules on the surface of S-CDs@Au NPs through the bonding between its primary amine with the carboxylic group of CDs and aggregation of DA-S-CDs@Au NPs by coordination of  $\text{Fe}^{3+}$  with DA molecules. In another study, Amirjani et al. [5] have proposed a rapid and sensitive colorimetric detection method for the determination of  $\text{Hg}^{2+}$  based on citrate-functionalized silver nanotriangles with a limit of detection of 4  $\text{nmol L}^{-1}$  which was below the safety level of  $\text{Hg}^{2+}$  ions (10  $\text{nmol L}^{-1}$ ) in drinking water. The ability of  $\text{Hg}^{2+}$  ion to interact with Ag and form the Hg-Ag alloy (amalgam) over the surface of nanotriangles resulted in an obvious color change from blue to violet. A comprehensive list of different organic compounds as functional ligand can be found in Table 4 [104–108].

Organic compounds include a large library of chemicals with the ability to link to plasmonic nanoparticles through S-H and  $\text{NH}_3$  linkage. One can simply choose the desired compound based on the required moiety for a specific analyte. Even though low detection limits can be obtained by this functionalization strategy, because the ligand is not specifically designed for the analyte the selectivity of the sensor is debatable.

## Conclusion and future prospects

During the last decade, many plasmonic sensors were designed and developed for a wide range of analytes from neurotransmitters to explosive chemicals [109–116]. The basis for their versatile applications is the sensitivity of localized plasmonic fields in the immediate vicinity of nanostructures. In this paper, recent advances in functionalization of plasmonic nanostructures for optical sensing were reviewed. With the emphasis on the nature of the functional ligands, they were categorized in four different groups namely as oligonucleotides, organic polymers, proteins and amino acids and organic compounds. Different scenarios for attachment of functional agents to NPs as well as different approaches for analyte chelation were reviewed and discussed in each category. Proper

functionalization of nanostructured probe is essential for selective determination of desired analyte. Engineered oligonucleotides as functional groups can be designed for selective determination of specific analytes with detection limit as low as  $\text{pM}$ . The efficiency and performance of plasmonic sensors are totally comparable or even superior to conventional detection methods. The ability of colorimetric detection in solution phase using plasmonic nanostructures makes the process rapid and straightforward. Nowadays, there is growing interest in immobilization of nanostructures on substrates (glass, paper, indium tin oxide (ITO), Polyethylene terephthalate (PET), etc.) for realization of lab-on-a-chip concept [117–119].

By immobilizing the nanostructured probe, sensors can be used for several detection cycles. In addition, there is a huge demand for using portable and easy accessible signal readers for such sensors such as smart phones instead of conventional spectrophotometers. The future prospect of plasmonic sensors is mainly dominated by immobilized NPs arrays on substrates, which are able to detect analytes on-site by the aid of a portable image analyzer unit (such as smartphones). These sensor arrays also make the multi-analyte determination possible by using different ligands for every specific analytes. In this decade, plasmonic sensors can become the gold standard for determination of chemical and biochemical species.

**Acknowledgments** Authors wish to dedicate this paper to Martyr Ali Akbar Shiroodi.

## Compliance with ethical standards

**Conflict of interest** The author(s) declare that they have no competing interests.

## References

1. Duan Z, Li Y, Zhang M, Bian H, Wang Y, Zhu L, Xia D (2020) Towards cleaner wastewater treatment for special removal of cationic organic dye pollutants: a case study on application of supramolecular inclusion technology with  $\beta$ -cyclodextrin derivatives. *J Clean Prod* 256:120308
2. Seleznev AA, Yarmoshenko IV, Malinovsky GP (2020) Urban geochemical changes and pollution with potentially harmful elements in seven Russian cities. *Sci Rep* 10(1):1–16
3. Zheng L, Jiao Y, Zhong H, Zhang C, Wang J, Wei Y (2020) Insight into the magnetic lime coagulation-membrane distillation process for desulfurization wastewater treatment: from pollutant removal feature to membrane fouling. *J Hazard Mater* 391:122202
4. Amirjani A, Haghshenas DF (2018) Ag nanostructures as the surface plasmon resonance (SPR) based sensors: a mechanistic study with an emphasis on heavy metallic ions detection. *Sensors Actuators B Chem* 273:1768–1779
5. Amirjani A, Haghshenas DF (2019) Facile and on-line colorimetric detection of  $\text{Hg}^{2+}$  based on localized surface plasmon resonance (LSPR) of Ag nanotriangles. *Talanta* 192:418–423
6. Bui HT, Lim JM, Mai DK, Kim H, Kim H-J, Kim HJ, Cho S (2020) Solvation and stabilization of ionic products of fluorescent

- water-content chemosensor in organic solvents. *Dyes Pigments* 176:108194
7. Geng Y, Peveler WJ, Rotello VM (2019) Array-based “chemical nose” sensing in diagnostics and drug discovery. *Angew Chem Int Ed* 58(16):5190–5200
  8. Xu Y, Kutsanedzie FY, Hassan M, Zhu J, Ahmad W, Li H, Chen Q (2020) Mesoporous silica supported orderly-spaced gold nanoparticles SERS-based sensor for pesticides detection in food. *Food Chem* 315:126300
  9. Xu Y, Zheng L, Yang C, Zheng W, Liu X, Zhang J (2020) Chemoresistive sensors based on Core-shell ZnO@ TiO<sub>2</sub> Nanorods designed by atomic layer deposition for n-butanol detection. *Sensors Actuators B Chem* 310:127846
  10. Luong HM, Pham MT, Madhogaria RP, Phan M-H, Larsen GK, Nguyen TD (2020) Bilayer Plasmonic Nano-lattices for tunable hydrogen sensing platform. *Nano energy* 71:104558
  11. Mauriz E, Dey P, Lechuga LM (2019) Advances in nanoplasmonic biosensors for clinical applications. *Analyst* 144(24):7105–7129
  12. Nan J, Zhu S, Ye S, Sun W, Yue Y, Tang X, Shi J, Xu X, Zhang J, Yang B (2020) Ultrahigh-sensitivity sandwiched plasmon ruler for label-free clinical diagnosis. *Adv Mater* 32(2):1905927
  13. Sergeev A, Pavlov D, Kuchmizhak A, Lapine M, Yiu W, Dong Y, Ke N, Juodkakis S, Zhao N, Kershaw S (2020) Tailoring spontaneous infrared emission of HgTe quantum dots with laser-printed plasmonic arrays. *Light Sci Appl* 9(1):1–10
  14. Vala M, Ertsgaard CT, Wittenberg NJ, Oh S-H (2019) Plasmonic sensing on symmetric nanohole arrays supporting high-Q hybrid modes and reflection geometry. *ACS sensors* 4(12):3265–3274
  15. Wang H, Chen W, Chen B, Jiao Y, Wang Y, Wang X, Du X, Hu Y, Lv X, Zeng Y (2020) Interfacial capillary-force-driven self-assembly of monolayer colloidal crystals for supersensitive Plasmonic sensors. *Small* 6:1905480
  16. Y-l L, Zhu J, G-j W, J-j L, J-w Z (2020) Gold nanotubes: synthesis, properties and biomedical applications. *Microchim Acta* 187: 612. <https://doi.org/10.1007/s00604-020-04460-y>
  17. Jia S, Li P, Koh K, Chen H (2016) A cytosensor based on NiO nanoparticle-enhanced surface plasmon resonance for detection of the breast cancer cell line MCF-7. *Microchim Acta* 183(2):683–688
  18. Chen W, Li J, Wei X, Fan Y, Qian H, Li S, Xiang Y, Ding S (2020) Surface plasmon resonance biosensor using hydrogel-AuNP supramolecular spheres for determination of prostate cancer-derived exosomes. *Microchim Acta* 187:187. <https://doi.org/10.1007/s00604-020-04573-4>
  19. Sun T, Zhang Y, Zhao F, Xia N, Liu L (2020) Self-assembled biotin-phenylalanine nanoparticles for the signal amplification of surface plasmon resonance biosensors. *Mikrochim Acta* 187(8): 473. <https://doi.org/10.1007/s00604-020-04461-x>
  20. Gao W, Li P, Qin S, Huang Z, Cao Y, Liu X (2019) A highly sensitive tetracycline sensor based on a combination of magnetic molecularly imprinted polymer nanoparticles and surface plasmon resonance detection. *Microchim Acta* 186:637. <https://doi.org/10.1007/s00604-019-3718-9>
  21. Namazi N, Rahbarimehr E, Amirjani A, Haghshenas Fatmehsari D (2020) Detection of cobalt ion based on surface Plasmon resonance of L-cysteine functionalized silver Nanotriangles. *Plasmonics*. <https://doi.org/10.1007/s11468-020-01289-2>
  22. Amirjani A, Koochak NN, Haghshenas DF (2019) Investigating the shape and size-dependent optical properties of silver nanostructures using UV–vis spectroscopy. *J Chem Educ* 96(11): 2584–2589
  23. Ross MB, Mirkin CA, Schatz GC (2016) Optical properties of one-, two-, and three-dimensional arrays of plasmonic nanostructures. *J Phys Chem C* 120(2):816–830
  24. Amirjani A, Koochak NN, Haghshenas DF (2018) Synthesis of silver nanotriangles with tunable edge length: a promising candidate for light harvesting purposes within visible and near-infrared ranges. *Mater Res Express* 6(3):036204. <https://doi.org/10.1088/2053-1591/aaf624>
  25. Lu X, Rycenga M, Skrabalak SE, Wiley B, Xia Y (2009) Chemical synthesis of novel plasmonic nanoparticles. *Annu Rev Phys Chem* 60:167–192
  26. Amirjani A, Firouzi F, Haghshenas DF (2020) Predicting the size of silver nanoparticles from their optical properties. *Plasmonics* 15(4):1077–1082. <https://doi.org/10.1007/s11468-020-01121-x>
  27. Mahmoud MA, Chamanzar M, Adibi A, El-Sayed MA (2012) Effect of the dielectric constant of the surrounding medium and the substrate on the surface Plasmon resonance Spectrum and sensitivity factors of highly symmetric systems: silver Nanocubes. *J Am Chem Soc* 134(14):6434–6442. <https://doi.org/10.1021/ja300901e>
  28. Novo C, Funston AM, Pastoriza-Santos I, Liz-Marzán LM, Mulvaney P (2008) Influence of the medium refractive index on the optical properties of single gold triangular prisms on a substrate. *J Phys Chem C* 112(1):3–7. <https://doi.org/10.1021/jp709606u>
  29. Daneshfar N, Foroughi H (2016) Optical bistability in plasmonic nanoparticles: effect of size, shape and embedding medium. *Physica E Low Dimens Syst Nanostruct* 83:268–274
  30. Jain PK, El-Sayed MA (2008) Noble metal nanoparticle pairs: effect of medium for enhanced Nanosensing. *Nano Lett* 8(12): 4347–4352. <https://doi.org/10.1021/nl8021835>
  31. Yan F, Jiang Y, Sun X, Bai Z, Zhang Y, Zhou X (2018) Surface modification and chemical functionalization of carbon dots: a review. *Microchim Acta* 185(9):424
  32. Panja AS, Maiti S, Bandyopadhyay B (2020) Protein stability governed by its structural plasticity is inferred by physicochemical factors and salt bridges. *Sci Rep* 10(1):1–9
  33. Sharma V, Yañez O, Alegría-Arcos M, Kumar A, Thakur RC, Cantero-López P (2020) A physicochemical and conformational study of co-solvent effect on the molecular interactions between similarly charged protein surfactant (BSA-SDBS) system. *J Chem Thermodyn* 142:106022
  34. Cagliani R, Gatto F, Bardi G (2019) Protein adsorption: a feasible method for nanoparticle functionalization? *Materials* 12(12):1991
  35. Dyawanapelly S, Mehrotra P, Ghosh G, Jagtap DD, Dandekar P, Jain R (2019) How the surface functionalized nanoparticles affect conformation and activity of proteins: exploring through protein-nanoparticle interactions. *Bioorg Chem* 82:17–25
  36. Di Marco M, Shamsuddin S, Razak KA, Aziz AA, Devaux C, Borghi E, Levy L, Sadun C (2010) Overview of the main methods used to combine proteins with nanosystems: absorption, bioconjugation, and encapsulation. *Int J Nanomedicine* 5:37
  37. Liao G, Liu X (2020) Surface plasmon resonance assay for exosomes based on aptamer recognition and polydopamine-functionalized gold nanoparticles for signal amplification. *Mikrochim Acta* 187(4):251. <https://doi.org/10.1007/s00604-020-4183-1>
  38. Wang S, Zhang H, Li W, Birech Z, Ma L, Li D, Li S, Wang L, Shang J, Hu J (2019) A multi-channel localized surface plasmon resonance system for absorptometric determination of abscisic acid by using gold nanoparticles functionalized with a polyadenine-tailed aptamer. *Microchim Acta* 187(1):20. <https://doi.org/10.1007/s00604-019-4003-7>
  39. Jeevika A, Shankaran DR (2016) Functionalized silver nanoparticles probe for visual colorimetric sensing of mercury. *Mater Res Bull* 83:48–55
  40. Zhao Q, Yan H, Liu P, Yao Y, Wu Y, Zhang J, Li H, Gong X, Chang J (2016) An ultra-sensitive and colorimetric sensor for

- copper and iron based on glutathione-functionalized gold nanoclusters. *Anal Chim Acta* 948:73–79
41. Ma Y, Pang Y, Liu F, Xu H, Shen X (2016) Microwave-assisted ultrafast synthesis of silver nanoparticles for detection of Hg<sup>2+</sup>. *Spectrochim Acta A Mol Biomol Spectrosc* 153:206–211
  42. Sang F, Li X, Zhang Z, Liu J, Chen G (2018) Recyclable colorimetric sensor of Cr<sup>3+</sup> and Pb<sup>2+</sup> ions simultaneously using a zwitterionic amino acid modified gold nanoparticles. *Spectrochim Acta A Mol Biomol Spectrosc* 193:109–116
  43. Buduru P, Reddy BSR, Naidu N (2017) Functionalization of silver nanoparticles with glutamine and histidine for simple and selective detection of Hg<sup>2+</sup> ion in water samples. *Sensors Actuators B Chem* 244:972–982
  44. Ermini ML, Chadtová Song X, Špringer T, Homola J (2019) Peptide functionalization of gold nanoparticles for the detection of carcinoembryonic antigen in blood plasma via SPR-based biosensor. *Front Chem* 7:40
  45. Satheshkumar E, Yang J, Srinivasadesikan V, Lin M-C (2017) Simultaneous production and surface functionalization of silver nanoparticles for label-free colorimetric detection of copper ion. *Anal Sci* 33(10):1115–1121
  46. D'souza SL, Pati R, Kailasa SK (2015) Ascorbic acid-functionalized Ag NPs as a probe for colorimetric sensing of glutathione. *Appl Nanosci* 5(6):747–753
  47. Batistela DM, Stevani CV, Freire RS (2017) Immunoassay for human IgG using antibody-functionalized silver nanoparticles. *Anal Sci* 33(10):1111–1114
  48. Beeg M, Nobili A, Orsini B, Rogai F, Gilardi D, Fiorino G, Danese S, Salmona M, Garattini S, Gobbi M (2019) A surface Plasmon resonance-based assay to measure serum concentrations of therapeutic antibodies and anti-drug antibodies. *Sci Rep* 9(1):1–9
  49. Hearty S, Leonard P, Ma H, O'Kennedy R (2018) Measuring antibody-antigen binding kinetics using surface Plasmon resonance. *Antibody Engineering*. Springer, In, pp 421–455
  50. Kim S, Lee HJ (2017) Gold nanostar enhanced surface plasmon resonance detection of an antibiotic at attomolar concentrations via an aptamer-antibody sandwich assay. *Anal Chem* 89(12):6624–6630
  51. Kim S, Park JW, Wark AW, Jhung SH, Lee HJ (2017) Tandem femto-and nanomolar analysis of two protein biomarkers in plasma on a single mixed antibody monolayer surface using surface plasmon resonance. *Anal Chem* 89(22):12562–12568
  52. Liu X, Marrakchi M, Xu D, Dong H, Andreescu S (2016) Biosensors based on modularly designed synthetic peptides for recognition, detection and live/dead differentiation of pathogenic bacteria. *Biosens Bioelectron* 80:9–16
  53. Wu B, Jiang R, Wang Q, Huang J, Yang X, Wang K, Li W, Chen N, Li Q (2016) Detection of C-reactive protein using nanoparticle-enhanced surface plasmon resonance using an aptamer-antibody sandwich assay. *Chem Commun* 52(17):3568–3571
  54. Yılmaz E, Özgür E, Bereli N, Türkmen D, Denizli A (2017) Plastic antibody based surface plasmon resonance nanosensors for selective atrazine detection. *Mater Sci Eng C* 73:603–610
  55. Zeinoddini M, Azizi A, Bayat S, Tavasoli Z (2018) Localized surface plasmon resonance (LSPR) detection of diphtheria toxin using gold nanoparticle-mono-clonal antibody conjugates. *Plasmonics* 13(2):583–590
  56. Kim D-Y, Shinde S, Ghodake G (2017) Colorimetric detection of magnesium (II) ions using tryptophan functionalized gold nanoparticles. *Sci Rep* 7(1):1–9
  57. Zhu R, Song J, Zhou Y, Lei P, Li Z, Li H-W, Shuang S, Dong C (2019) Dual sensing reporter system of assembled gold nanoparticles toward the sequential colorimetric detection of adenosine and Cr (III). *Talanta* 204:294–303
  58. Busayapongchai P, Siri S (2017) Sensitive detection of estradiol based on ligand binding domain of estrogen receptor and gold nanoparticles. *Anal Biochem* 518:60–68
  59. Jia F, Liu Q, Wei W, Chen Z (2019) Colorimetric sensor assay for discrimination of proteins based on exonuclease I-triggered aggregation of DNA-functionalized gold nanoparticles. *Analyst* 144(16):4865–4870
  60. Chu J, Park C, Jang K, Shim JH, Na S (2018) A technique for highly sensitive detection of mercury ions using DNA-functionalized gold nanoparticles and resonators based on a resonance frequency shift. *J Mech Sci Technol* 32(2):799–804
  61. Quintela I, de los Reyes B, Lin C-S, Wu VC (2019) Simultaneous colorimetric detection of a variety of Salmonella spp. in food and environmental samples by optical biosensing using oligonucleotide-gold nanoparticles. *Front Microbiol* 10:1138
  62. Zou L, Li R, Zhang M, Luo Y, Zhou N, Wang J, Ling L (2017) A colorimetric sensing platform based upon recognizing hybridization chain reaction products with oligonucleotide modified gold nanoparticles through triplex formation. *Nanoscale* 9(5):1986–1992
  63. Alkilany AM, Abulateefeh SR, Murphy CJ (2019) Facile functionalization of gold nanoparticles with PLGA polymer brushes and efficient encapsulation into PLGA nanoparticles: toward spatially precise bioimaging of polymeric nanoparticles. *Part Part Syst Charact* 36(2):1800414
  64. Galati E, Tebbe M, Querejeta-Fernández A, Xin HL, Gang O, Zhulina EB, Kumacheva E (2017) Shape-specific patterning of polymer-functionalized nanoparticles. *ACS Nano* 11(5):4995–5002
  65. Huang Q, Liu M, Mao L, Xu D, Zeng G, Huang H, Jiang R, Deng F, Zhang X, Wei Y (2017) Surface functionalized SiO<sub>2</sub> nanoparticles with cationic polymers via the combination of mussel inspired chemistry and surface initiated atom transfer radical polymerization: characterization and enhanced removal of organic dye. *J Colloid Interface Sci* 499:170–179
  66. Maruthupandy M, Rajivgandhi G, Muneeswaran T, Vennila T, Quero F, Song J-M (2019) Chitosan/silver nanocomposites for colorimetric detection of glucose molecules. *Int J Biol Macromol* 121:822–828
  67. Amirjani A, Bagheri M, Heydari M, Hesaraki S (2016) Colorimetric determination of Timolol concentration based on localized surface plasmon resonance of silver nanoparticles. *Nanotechnology* 27(37):375503
  68. Vasileva P, Alexandrova T, Karadjova I (2017) Application of starch-stabilized silver nanoparticles as a colorimetric sensor for mercury (II) in 0.005 Mol/L nitric acid. *J Chemother* 2017:6897960
  69. Buccolieri A, Serra A, Giancane G, Manno D (2018) Colloidal solution of silver nanoparticles for label-free colorimetric sensing of ammonia in aqueous solutions. *Beilstein J Nanotechnol* 9(1):499–507
  70. Ban DK, Paul S (2018) Rapid colorimetric and spectroscopy based sensing of heavy metal and cellular free oxygen radical by surface functionalized silver nanoparticles. *Appl Surf Sci* 458:245–251
  71. J-j L, Wang X-f, D-q H, C-j H, H-b F, Yang M, Zhang L (2017) Colorimetric measurement of Fe<sup>3+</sup> using a functional paper-based sensor based on catalytic oxidation of gold nanoparticles. *Sensors Actuators B Chem* 242:1265–1271
  72. Shi X, Lu D, Wang Z, Zhang D, Gao W, Zhang C, Deng J, Guo S (2018) Colorimetric and visual determination of acrylamide via acrylamide-mediated polymerization of acrylamide-functionalized gold nanoparticles. *Microchim Acta* 185(11):522. <https://doi.org/10.1007/s00604-018-3062-5>
  73. Liu Y, Dai J, Xu L, Liu X, Liu J, Li G (2016) Red to brown to green colorimetric detection of Ag<sup>+</sup> based on the formation of au-



- Ag core-shell NPs stabilized by a multi-sulphydryl functionalized hyperbranched polymer. *Sensors Actuators B Chem* 237:216–223. <https://doi.org/10.1016/j.snb.2016.06.096>
74. Teodoro KBR, Migliorini FL, Christinelli WA, Correa DS (2019) Detection of hydrogen peroxide (H<sub>2</sub>O<sub>2</sub>) using a colorimetric sensor based on cellulose nanowhiskers and silver nanoparticles. *Carbohydr Polym* 212:235–241. <https://doi.org/10.1016/j.carbpol.2019.02.053>
75. Faghiri F, Ghorbani F (2019) Colorimetric and naked eye detection of trace Hg<sup>2+</sup> ions in the environmental water samples based on plasmonic response of sodium alginate impregnated by silver nanoparticles. *J Hazard Mater* 374:329–340. <https://doi.org/10.1016/j.jhazmat.2019.04.052>
76. Marimuthu V, Chandrasekar S, Rajendiran N (2018) Green synthesis of sodium Cholate stabilized silver nanoparticles: an effective colorimetric sensor for Hg<sup>2+</sup> and Pb<sup>2+</sup> ions. *ChemistrySelect* 3(14):3918–3924. <https://doi.org/10.1002/slct.201800219>
77. Pai J-H, Yang C-T, Hsu H-Y, Wedding AB, Thierry B (2017) Development of a simplified approach for the fabrication of localized surface plasmon resonance sensors based on gold nanorods functionalized using mixed polyethylene glycol layers. *Anal Chim Acta* 974:87–92
78. Halkare P, Punjabi N, Wangchuk J, Nair A, Kondabagil K, Mukherji S (2019) Bacteria functionalized gold nanoparticle matrix based fiber-optic sensor for monitoring heavy metal pollution in water. *Sensors Actuators B Chem* 281:643–651
79. Amirjani A, Fatmehsari DH (2018) Colorimetric detection of ammonia using smartphones based on localized surface plasmon resonance of silver nanoparticles. *Talanta* 176:242–246
80. Zheng M, Wang Y, Wang C, Wei W, Ma S, Sun X, He J (2018) Silver nanoparticles-based colorimetric array for the detection of Thiophanate-methyl. *Spectrochim Acta A Mol Biomol Spectrosc* 198:315–321
81. Mehta VN, Rohit JV, Kailasa SK (2016) Functionalization of silver nanoparticles with 5-sulfoanthranilic acid dithiocarbamate for selective colorimetric detection of Mn<sup>2+</sup> and Cd<sup>2+</sup> ions. *New J Chem* 40(5):4566–4574
82. Song J, Wu F, Wan Y, Ma L (2015) Colorimetric detection of melamine in pretreated milk using silver nanoparticles functionalized with sulfanilic acid. *Food Control* 50:356–361
83. Patel GM, Rohit JV, Singhal RK, Kailasa SK (2015) Recognition of carbendazim fungicide in environmental samples by using 4-aminobenzenethiol functionalized silver nanoparticles as a colorimetric sensor. *Sensors Actuators B Chem* 206:684–691
84. Devadiga A, Shetty KV, Saidutta M (2017) Highly stable silver nanoparticles synthesized using *Terminalia catappa* leaves as antibacterial agent and colorimetric mercury sensor. *Mater Lett* 207:66–71
85. Amirjani A, Bagheri M, Heydari M, Hesarakhi S (2016) Label-free surface plasmon resonance detection of hydrogen peroxide; a bio-inspired approach. *Sensors Actuators B Chem* 227:373–382
86. Ismail M, Khan M, Akhtar K, Ali M, Asiri A, Bahadar S (2018) *Physica e: low-dimensional systems and nanostructures biosynthesis of silver nanoparticles: a colorimetric optical sensor for detection of hexavalent chromium and ammonia in aqueous solution*. *Physica E Low Dimens Syst Nanostruct* 103:367–376
87. Uddin I, Ahmad K, Khan AA, Kazmi MA (2017) Synthesis of silver nanoparticles using *Matricaria recutita* (Babunah) plant extract and its study as mercury ions sensor. *Sens Bio-Sensing Res* 16:62–67
88. Muthivhi R, Parani S, May B, Oluwafemi OS (2018) Green synthesis of gelatin-noble metal polymer nanocomposites for sensing of Hg<sup>2+</sup> ions in aqueous media. *Nano-Struct Nano-Objects* 13:132–138
89. Pinyorosphum C, Rattanarat P, Chaiyo S, Siangproh W, Chailapakul O (2019) Colorimetric sensor for determination of phosphate ions using anti-aggregation of 2-mercaptoethanesulfonate-modified silver nanoplates and europium ions. *Sensors Actuators B Chem* 290:226–232
90. Chen Z, Hu Y, Yang Q, Wan C, Tan Y, Ma H (2015) A highly sensitive colorimetric sensor for adrenaline detection based on organic molecules-functionalized gold nanoparticles. *Sensors Actuators B Chem* 207:277–280
91. Khodaveisi J, Shabani AMH, Dadfarnia S, Saberi D (2017) A novel sensor for determination of naproxen based on change in localized surface plasmon peak of functionalized gold nanoparticles. *Spectrochim Acta A Mol Biomol Spectrosc* 179:11–16
92. Qin L, Zeng G, Lai C, Huang D, Zhang C, Xu P, Hu T, Liu X, Cheng M, Liu Y (2017) A visual application of gold nanoparticles: simple, reliable and sensitive detection of kanamycin based on hydrogen-bonding recognition. *Sensors Actuators B Chem* 243:946–954
93. Khodaveisi J, Dadfarnia S, Shabani AMH, Saberi D (2017) Colorimetric determination of nabumetone based on localized surface plasmon resonance of functionalized gold nanoparticles as a chemical sensor. *Sensors Actuators B Chem* 239:1300–1306
94. Chen Y, Han S, Yang S, Pu Q (2017) Rhodanine stabilized gold nanoparticles for sensitive and selective detection of mercury (II). *Dyes Pigments* 142:126–131
95. Scaglione F, Alladio E, Damin A, Turci F, Baggiani C, Giovannoli C, Bordiga S, Battezzati L, Rizzi P (2019) Functionalized nanoporous gold as a new biosensor platform for ultra-low quantitative detection of human serum albumin. *Sensors Actuators B Chem* 288:460–468
96. Kailasa SK, Nguyen TP, Baek SH, Rafique R, Park TJ (2019) Assembly of 6-aza-2-thiothymine on gold nanoparticles for selective and sensitive colorimetric detection of pencycuron in water and food samples. *Talanta* 205:120087
97. Tian Y, Liu Q, Jiao Y, Jia R, Chen Z (2018) Colorimetric aggregation based cadmium (II) assay by using triangular silver nanoplates functionalized with 1-amino-2-naphthol-4-sulfonate. *Microchim Acta* 185(1):6
98. Piotrowski P, Bukowska J (2015) 2-Mercaptoethanesulfonate (MES) anion-functionalized silver nanoparticles as an efficient SERS-based sensor of metal cations. *Sensors Actuators B Chem* 221:700–707
99. Detsri E, Seeharaj P, Sriwong C (2018) A sensitive and selective colorimetric sensor for reduced glutathione detection based on silver triangular nanoplates conjugated with gallic acid. *Colloids Surf A Physicochem Eng Asp* 541:36–42
100. Mochi F, Burratti L, Fratoddi I, Venditti I, Battocchio C, Carlini L, Iucci G, Casalboni M, De Matteis F, Casciardi S (2018) Plasmonic sensor based on interaction between silver nanoparticles and Ni<sup>2+</sup> or Co<sup>2+</sup> in water. *Nanomaterials* 8(7):488
101. Lentka Ł, Kotarski M, Smulko J, Cindemir U, Topalian Z, Granqvist CG, Calavia R, Ionescu R (2016) Fluctuation-enhanced sensing with organically functionalized gold nanoparticle gas sensors targeting biomedical applications. *Talanta* 160:9–14
102. Buduru P (2016) Oxamic acid and p-aminobenzoic acid functionalized gold nanoparticles as a probe for colorimetric detection of Fe<sup>3+</sup> ion. *Sensors Actuators B Chem* 237:935–943
103. Amiri M, Dadfarnia S, Shabani AMH, Sadjadi S (2019) Non-enzymatic sensing of dopamine by localized surface plasmon resonance using carbon dots-functionalized gold nanoparticles. *J Pharm Biomed Anal* 172:223–229
104. Tao Y, Li M, Kim B, Auguste DT (2017) Incorporating gold nanoclusters and target-directed liposomes as a synergistic amplified colorimetric sensor for HER2-positive breast cancer cell detection. *Theranostics* 7(4):899–911. <https://doi.org/10.7150/thno.17927>



105. Nsengiyuma G, Hu R, Li J, Li H, Tian D (2016) Self-assembly of 1,3-alternate calix[4]arene carboxyl acids-modified silver nanoparticles for colorimetric Cu<sup>2+</sup> sensing. *Sensors Actuators B Chem* 236:675–681. <https://doi.org/10.1016/j.snb.2016.05.148>
106. Bhattacharjee Y, Chatterjee D, Chakraborty A (2018) Mercaptobenzoheterocyclic compounds functionalized silver nanoparticle, an ultrasensitive colorimetric probe for hg(II) detection in water with picomolar precision: a correlation between sensitivity and binding affinity. *Sensors Actuators B Chem* 255: 210–216. <https://doi.org/10.1016/j.snb.2017.08.066>
107. Boruah BS, Daimari NK, Biswas R (2019) Functionalized silver nanoparticles as an effective medium towards trace determination of arsenic (III) in aqueous solution. *Results Phys* 12:2061–2065. <https://doi.org/10.1016/j.rinp.2019.02.044>
108. Vyas G, Bhatt S, Paul P (2019) Synthesis of Calixarene-capped silver nanoparticles for colorimetric and Amperometric detection of mercury (HgII, Hg0). *ACS Omega* 4(2):3860–3870. <https://doi.org/10.1021/acsomega.8b03299>
109. Wang J, Muto M, Yatabe R, Tahara Y, Onodera T, Tanaka M, Okochi M, Toko K (2018) Highly selective rational Design of Peptide-Based Surface Plasmon Resonance Sensor for direct determination of 2,4,6-trinitrotoluene (TNT) explosive. *Sensors Actuators B Chem* 264:279–284. <https://doi.org/10.1016/j.snb.2018.02.075>
110. Wang J, Muto M, Yatabe R, Onodera T, Tanaka M, Okochi M, Toko K (2017) Rational design of peptide-functionalized surface plasmon resonance sensor for specific detection of TNT explosive. *Sensors* 17(10):2249
111. Wang J, Du S, Onodera T, Yatabe R, Tanaka M, Okochi M, Toko K (2018) An SPR sensor chip based on peptide-modified single-walled carbon nanotubes with enhanced sensitivity and selectivity in the detection of 2, 4, 6-trinitrotoluene explosives. *Sensors* 18(12):4461
112. Milkani E, Lambert CR, McGimpsey WG (2011) Direct detection of acetylcholinesterase inhibitor binding with an enzyme-based surface plasmon resonance sensor. *Anal Biochem* 408(2):212–219. <https://doi.org/10.1016/j.ab.2010.09.009>
113. Pathak A, Gupta BD Fiber Optic Plasmonic Sensor Utilizing Carbon Nanotubes Based Surface Imprinted Matrix for the Sensing of Dopamine. In: 2018 Conference on Lasers and Electro-Optics Pacific Rim (CLEO-PR), 29 July-3 Aug. 2018 2018. pp 1–2
114. Kant R, Gupta BD (2018) Fiber-optic SPR based acetylcholine biosensor using enzyme functionalized Ta2O5 Nanoflakes for Alzheimer's disease diagnosis. *J Lightwave Technol* 36(18): 4018–4024. <https://doi.org/10.1109/JLT.2018.2856924>
115. Jafarinejad S, Ghazi-Khansari M, Ghasemi F, Sasanpour P, Hormozi-Nezhad MR (2017) Colorimetric fingerprints of gold Nanorods for discriminating catecholamine neurotransmitters in urine samples. *Sci Rep* 7(1):8266. <https://doi.org/10.1038/s41598-017-08704-5>
116. Atar N, Eren T, Yola ML, Wang S (2015) A sensitive molecular imprinted surface plasmon resonance nanosensor for selective determination of trace triclosan in wastewater. *Sensors Actuators B Chem* 216:638–644. <https://doi.org/10.1016/j.snb.2015.04.076>
117. Wang Y, Li D, Sun Y, Zhong L, Liang W, Qin W, Guo W, Liang Z, Jiang L (2020) Multiplexed assembly of Plasmonic nanostructures through charge inversion on substrate for surface encoding. *ACS Appl Mater Interfaces* 12(5):6176–6182. <https://doi.org/10.1021/acsami.9b17530>
118. Golze SD, Hughes RA, Rouvimov S, Neal RD, Demille TB, Neretina S (2019) Plasmon-mediated synthesis of periodic arrays of gold Nanoplates using substrate-immobilized seeds lined with planar defects. *Nano Lett* 19(8):5653–5660. <https://doi.org/10.1021/acs.nanolett.9b02215>
119. Demille TB, Hughes RA, Neretina S (2019) Periodic arrays of Dewetted silver nanostructures on sapphire and quartz: effect of substrate truncation on the localized surface Plasmon resonance and near-field enhancement. *J Phys Chem C* 123(32):19879–19886. <https://doi.org/10.1021/acs.jpcc.9b05692>

**Publisher's note** Springer Nature remains neutral with regard to jurisdictional claims in published maps and institutional affiliations.